



**HAL**  
open science

## A multilevel approach to cancer growth modeling

P.P. Delsanto, C.A. Condat, N. Pugno, A.S. Gliozzi, M. Griffa

► **To cite this version:**

P.P. Delsanto, C.A. Condat, N. Pugno, A.S. Gliozzi, M. Griffa. A multilevel approach to cancer growth modeling. *Journal of Theoretical Biology*, 2009, 250 (1), pp.16. 10.1016/j.jtbi.2007.09.023 . hal-00554497

**HAL Id: hal-00554497**

**<https://hal.science/hal-00554497>**

Submitted on 11 Jan 2011

**HAL** is a multi-disciplinary open access archive for the deposit and dissemination of scientific research documents, whether they are published or not. The documents may come from teaching and research institutions in France or abroad, or from public or private research centers.

L'archive ouverte pluridisciplinaire **HAL**, est destinée au dépôt et à la diffusion de documents scientifiques de niveau recherche, publiés ou non, émanant des établissements d'enseignement et de recherche français ou étrangers, des laboratoires publics ou privés.

## Author's Accepted Manuscript

A multilevel approach to cancer growth modeling

P.P. Delsanto, C.A. Condat, N. Pugno, A.S. Gliozzi,  
M. Griffa

PII: S0022-5193(07)00452-3  
DOI: doi:10.1016/j.jtbi.2007.09.023  
Reference: YJTBI 4861

To appear in: *Journal of Theoretical Biology*

Received date: 10 January 2007  
Revised date: 18 September 2007  
Accepted date: 18 September 2007

Cite this article as: P.P. Delsanto, C.A. Condat, N. Pugno, A.S. Gliozzi and M. Griffa, A multilevel approach to cancer growth modeling, *Journal of Theoretical Biology* (2007), doi:10.1016/j.jtbi.2007.09.023

This is a PDF file of an unedited manuscript that has been accepted for publication. As a service to our customers we are providing this early version of the manuscript. The manuscript will undergo copyediting, typesetting, and review of the resulting galley proof before it is published in its final citable form. Please note that during the production process errors may be discovered which could affect the content, and all legal disclaimers that apply to the journal pertain.



[www.elsevier.com/locate/jtbi](http://www.elsevier.com/locate/jtbi)

# A multilevel approach to cancer growth modeling

P.P. Delsanto <sup>a,1,\*</sup>, C.A. Condat <sup>c</sup>, N. Pugno <sup>b</sup>,

A.S. Gliozzi <sup>a</sup>, M. Griffa <sup>d,1</sup>

<sup>a</sup>*Dept. of Physics, Politecnico di Torino, Corso Duca degli Abruzzi 24, 10129  
Torino, Italy*

<sup>b</sup>*Dept. of Structural Engineering, Politecnico di Torino, Corso Duca degli Abruzzi  
24, 10129 Torino, Italy*

<sup>c</sup>*CONICET and FaMAF, Universidad Nacional de Córdoba, 5000-Córdoba,  
Argentina*

<sup>d</sup>*EES-11, MS D443, Los Alamos National Laboratory, Los Alamos, New Mexico,  
USA*

---

## Abstract

Cancer growth models may be divided into macroscopic models, which describe the tumor as a single entity, and microscopic ones, which consider the tumor as a complex system whose behaviour emerges from the local dynamics of its basic components, the neoplastic cells. Mesoscopic models (e.g. as based on the Local Interaction Simulation Approach (Delsanto et al., 1998)), which explicitly consider the behavior of cell clusters and their interactions, may be used instead of the microscopic ones, in order to study the properties of cancer biology that strongly depend on the interactions of small groups of cells at intermediate spatial and temporal scales. All these approaches have been developed independently, which

limits their usefulness, since they all include relevant features and information that should be cross-correlated for a deeper understanding of the mechanisms involved.

In this contribution we consider multicellular tumor spheroids as biological reference systems and propose an intermediate model to bridge the gap between a macroscopic formulation of tumor growth and a mesoscopic one. Thus we are able to establish, as an important result of our formalism, a direct correspondence between parameters characterizing processes occurring at different scales. In particular, we analyze their dependence on an important limiting factor to tumor growth, i.e. the extra-cellular matrix pressure. Since the macro and meso-models stem from totally different roots (energy conservation and clinical observations vs cell groups dynamics), their consistency may be used to validate both approaches. It may also be interesting to note that the proposed formalism fits well into a recently proposed conjecture of growth laws universality.

*Key words:* Cancer growth, Multicellular Tumor Spheroids, Modeling, Scaling, Multilevel Approach, Cellular Dynamics, Universality, Energy Balance, Complexity

*PACS:* 87.17.Aa, 05.65.+b, 87.18.Bb, 89.75.Da

---

\* Corresponding author: Tel. +39 0115647320. Fax +39 0115647399

*Email addresses:* pier.delsanto@polito.it (P.P. Delsanto),  
condat@famaf.unc.edu.ar (C.A. Condat), nicola.pugno@polito.it (N.  
Pugno), antonio.gliozi@polito.it (A.S. Gliozzi), mgriffa@lanl.gov (M.  
Griffa).

<sup>1</sup> Also at: Bioinformatics and High Performance Computing Lab, Bioindustry Park of Canavese, Via Ribes 5, 10100, Colletterto Giacosa (TO), Italy

## 1 INTRODUCTION

2 Crucial to our understanding of the development of complexity is our ability  
3 to relate phenomena occurring at different scales. This is necessary not only to  
4 predict the emergence of macroscopic phenomena from microscopic processes,  
5 but also to relate microscopic variables to the more accessible parameters of  
6 macroscopic phenomenology. In fact, the use of more realistic values for the pa-  
7 rameters of the microscopic (and mesoscopic) simulations may greatly enhance  
8 their predictive potentiality and, therefore, their applicability for biomedical  
9 clinical purposes. As a rule, numerical simulations are necessary to imple-  
10 ment microscopic or mesoscopic models, while analytical (or semi-analytical)  
11 solutions are usually possible for macroscopic models.

12 Tumors are remarkable examples of complex self-organizing systems. Due  
13 to their inherent complexity, it is necessary to analyze their growth at dif-  
14 ferent scales. In a macroscopic approach, we consider them as single entities,  
15 whose behavior can be predicted in terms of their global interaction with the  
16 environment and a few internal parameters. This approach has led to a host  
17 of useful models of cellular population dynamics in different biological sys-  
18 tems (for example cell cultures (Murray, 2004), the immune system (Adam  
19 and Bellomo, 1996; Perelson and Weisbuch, 1997), neoplastic masses (Adam  
20 and Bellomo, 1996; Preziosi, 2003)).

21 Interest in this approach has been further rekindled by the conjecture of  
22 Guiot et al. (Guiot et al., 2003) that the ontogenetic growth law for all living  
23 organisms of West, Brown, and Enquist (WBE) (West et al., 1999, 2001) may  
24 be fruitfully extended to cancer growth. In the form proposed by WBE, this  
25 law states that two hypotheses suffice to ensure the existence of a universal  
26 growth dynamics: the conservation of energy and the presence of a fractal

27 distribution network for energy supply at each part of the biological system  
28 considered. These basic hypotheses lead to the well-known exponent in the  
29 relationship between metabolic rate and mass scaling, which is purportedly  
30 characteristic of all organisms.

31 In a *microscopic* description, one should identify individual cell properties  
32 and predict tumor development from cell-cell interactions. Such an approach  
33 has two drawbacks: first, cancer growth is a collective phenomenon whose  
34 complexity may not emerge from the ensemble of its individual cell properties  
35 alone. Second, the huge number of cells involved (typically  $10^8$  cells for a  $1\text{ cm}^3$   
36 tumor) restricts considerably the feasibility of simulations taking into account  
37 the behavior and dynamics of each individual cell, unless populations with a  
38 small number of individuals can be considered. As a consequence, *mesoscopic*  
39 models (Scalerandi et al., 1999; Scalerandi et al., 2001b; Sansone et al., 2001a;  
40 Ferreira et al., 2002; Scalerandi et al., 2002; Scalerandi and Sansone, 2002;  
41 Chen et al., 2003) have been proposed, in which the coarse graining of the  
42 system, and the behavior of cell clusters and their interactions is considered.  
43 Mesoscopic models are also better adapted to describe the influence of the  
44 macroscale world on microscale phenomena and viceversa. A nice exposition  
45 of the insights that mathematical modeling can yield about the mechanisms  
46 underpinning the great complexity of the various phases of cancer growth is  
47 presented in a recent review by Byrne *et al.* (Byrne et al., 2006). Among other  
48 recent papers about modeling tumor growth, we can quote another review  
49 paper by Alarcón *et al.* (Alarcón et al., 2005) or, more generally, refer to the  
50 repository of mathematical models and corresponding computational codes  
51 assembled within the framework of the **CViT** (**C**enter for the development of  
52 a **V**irtual **T**umor) Project (<http://www.cvit.org>), belonging to the US NIH-  
53 NCI **ICBP** (**I**ntegrative **C**ancer **B**iology **P**rogram).

54 Multicellular Tumor Spheroids (MTSs) represent convenient experimental  
55 systems for analyzing and comparing tumor growth models at different lev-  
56 els. They are spherical aggregations of tumor cells that may be grown *in*  
57 *vitro* under strictly controlled conditions, mimicking some of the important  
58 features of solid tumors developing *in vivo* (Hamilton, 1998; Thomson and  
59 Byrne, 1999; Mueller-Klieser, 2000; Chignola et al., 2000; Kelm et al., 2003).  
60 Due to their simple geometry, the possibility of culturing them in large quan-  
61 tities and of controlling relevant parameters, such as the porosity and stiffness  
62 of the surrounding environment, they are excellent systems upon which to  
63 test the applicability of various models (Marusic et al., 1994; Delsanto et al.,  
64 2004, 2005a). Experimental spheroid setups are designed to provide a suitable  
65 amount of oxygen and other nutrients, which diffuse to the outer edges of  
66 the MTS, and then to the interior. Due to consumption by the outer region,  
67 nutrient concentration decreases towards the center. Consequently, as it has  
68 been observed, proliferating cells are usually present in the outermost shell,  
69 quiescent (non reproductive) cells dominate in the interior, and, eventually at  
70 a later stage of growth, a necrotic core is formed by dead cells. An MTS is  
71 thus an heterogeneous cellular system of considerable complexity, but whose  
72 properties and growth can be carefully monitored and modeled.

73 Using MTS's as working models (but with the expectation that our con-  
74 clusions may be applied also to the study of some aspects of *in vivo* tumor  
75 growth), we review in Sections 2 and 3 two recently proposed growth mod-  
76 els at the mesoscopic (Delsanto et al., 2005b) and macroscopic (Guiot et al.,  
77 2003; Delsanto et al., 2004) levels, respectively. The latter is extended in order  
78 to take into account the pressure exerted by the growing tumor against its  
79 environment. This term plays a crucial role in the mechanisms involved in  
80 tumoral invasion (Guiot et al., 2006b), which ultimately represents the proce-

81 dure which allows further growth of tumors *in vivo*. Then, in Sec. 4, we show  
 82 that it is possible to formulate a coherent picture embodying both descriptions  
 83 by means of an Intermediate Model (IM) (Delsanto et al., 2005a). A detailed  
 84 description of the IM and of the relationship (mediated by the IM) between  
 85 the mesoscopic and macroscopic parameters represents the main goal of the  
 86 present contribution.

## 87 2 A LINK TO CELL DYNAMICS: MESOSCOPIC MODEL

88 In this Section we review the mesoscopic MTS model of Ref. (Delsanto  
 89 et al., 2005b). In this model space is divided into concentric isovolumetric  
 90 shells  $n = 0, \dots, N$  ( $n = 0$  labels the central sphere of radius  $r_0$ ). Each shell  
 91 has a volume  $V_0 = (4/3)\pi r_0^3$ , and a correspondence is established between  
 92 the shell system and a one-dimensional grid. The center of the shell system  
 93 coincides with the location of the implanted spheroid seed. The MTS growth is  
 94 controlled by local nutrient availability and proceeds according to the following  
 95 rules (see Fig. 1):

96 a) Feeding: nutrient is absorbed by each shell at a rate  $\gamma c_n$ , where  $c_n$  is the  
 97 number of live cancer cells in the  $n^{\text{th}}$  shell.

98 b) Reproduction: cancer cells reproduce at rates  $\rho_n c_n$ , only in the shells  
 99 where the number  $\nu_n$  of locally available nutrient units exceeds a given thresh-  
 100 old  $Q_R$ .

101 c) Migration: cells migrate to adjacent shells with a flux  $\mu_n c_n$  per unit of  
 102 grid cell surface if the number of nutrient units falls below a threshold  $Q_M$ .

103 Since nutrients diffuse inwards, migration will usually proceed towards outer  
 104 shells. We may plausibly assume that outwards migration is also favored by  
 105 mechanical stress gradients (Gordon et al., 2003). Due to the bias introduced

106 by the radial gradients, we distinguish between outwards ( $\mu^+$ ) and inwards  
107 ( $\mu^-$ ) migration fluxes.

108 d) Death: cell death occurs (at rates  $\delta_n c_n$ ) where the number of nutrient  
109 units falls below the threshold  $Q_D$ .

110 The thresholds satisfy the conditions  $Q_D < Q_M < Q_R$ . Figure 1 sum-  
111 marizes in a simple scheme the set of thresholds associated to the different  
112 biological/biophysical phenomena and the corresponding value ranges for the  
113 rates. As reported in (Griffa et al., 2004) the actual implementation of the  
114 model makes use of sigmoidal functions for representing the rates dependence  
115 on nutrient concentration instead of Heaviside functions (i.e. thresholds).

116 Nutrients diffuse from the  $n^{\text{th}}$  shell to the adjacent ones at a rate  $\alpha \nu_n$  per  
117 unit area. Since cellular displacement and molecular diffusion between shells  
118 are proportional to the areas of the separating surfaces, the diffusion terms  
119 across the interface between the  $(n-1)$ -th and  $n$ -th shells will be proportional  
120 to  $n^{2/3}$ . The model equations are then written directly in their time-discretized  
121 forms:

$$c_n^* = c_n(1 - \tau\delta_n + \tau\rho_n) + \tau r_0^2 [n^{2/3}(\mu_{n-1}^+ c_{n-1} - \mu_n^- c_n) + (n+1)^{2/3}(\mu_{n+1}^- c_{n+1} - \mu_n^+ c_n)], \quad (1)$$

$$d_n^* = d_n + \tau\delta_n c_n - \tau\lambda_n d_n, \quad (2)$$

$$\nu_n^* = \nu_n - \tau\gamma c_n + \tau\alpha r_0^2 [n^{2/3}(\nu_{n-1} - \nu_n) + (n+1)^{2/3}(\nu_{n+1} - \nu_n)], \quad (3)$$

122 where  $\tau$  is the time step and the asterisk means that the corresponding  
123 quantity must be evaluated at the time  $t + \tau$ , instead of at the time  $t$ . In  
124 Eq.(2)  $d_n$  is the number of dead cells in the  $n^{\text{th}}$  shell; the last term, with a  
125 coefficient  $\lambda_n$ , has been added to account for possible disintegration of dead  
126 cells releasing intracellular fluid (Frieboes et al., 2006).

127 Numerical simulations based on the above model show that, in agreement  
128 with experimental observations, in a first stage the spheroid is fully populated

129 by proliferating cells. Then, in the inside, cells become quiescent, i.e. alive but  
130 not proliferating, with a “wavefront” of proliferating cells which have greater  
131 probability of undergoing an outward migration due to the second type of  
132 movement mechanism implemented in the model, the one based on a smoothed  
133 cell density-per each shell threshold, as explained in Ref. (Griffa et al., 2004).  
134 This *in silico* mechanism corresponds to the biomechanical stress-mediated  
135 transport of cells towards regions with lower levels of cell density, packing and  
136 deformation, due to both passive (purely elastic) and cell-mediated responses  
137 (Vernon et al., 1992; Dembo and Wang, 1999; Gordon et al., 2003; Deisboeck  
138 et al., 2005) to mechanical deformations. Finally, at later times, a predomi-  
139 nantly necrotic core develops. According to the model implementation, when  
140 the total number of living-plus-dead cells in the  $n$ -th shell is larger than a  
141 given threshold, the probability per unit of time of migration towards the  
142 nearest neighbor shells arises, so that some cells leave that shell. The thresh-  
143 old value is a function of the cell mean radius and of  $r_0$ . Thus, the mechanical  
144 stress-driven migration is essentially triggered by the unbalance between the  
145 volume of each shell and the one occupied by the living and dead cells. If  
146 the latter is too large, a higher level of packing and cell deformation occurs  
147 with mass transport as consequence. Different weights are assigned in com-  
148 puting the volume occupied by the living vs. dead cells, in order to account  
149 for their different deformation. Also, a rigid Heaviside function is replaced by  
150 a sigmoid. See Ref. (Griffa et al., 2004) for the mathematical details. Figure 2  
151 shows the radial distribution of viable cells within the simulated spheroid at  
152 three different time steps belonging respectively to the three cited stages of  
153 growth. The simulation aims at reproducing the typical layout of an MTS in  
154 terms of cell state spatial distribution.

155 **3 A LINK TO PHENOMENOLOGY: MACROSCOPIC MODEL**

156 Both the discussion in the Introduction and Fig. 2 suggest the use of a three-  
 157 layer macroscopic model for the tumor. Using the WBE model, as extended  
 158 to tumors in Ref. (Guiot et al., 2003), we assume that a central core of dead  
 159 cells (region  $Z_0$ ) is surrounded by a first layer  $Z_1$  of quiescent cells, and by an  
 160 outer layer  $Z_2$  of active cells and neglect, as temporary, any mixing, i.e. the  
 161 presence of cells in the “wrong” regions. We label the three cell species 0, 1,  
 162 and 2 respectively, and call their corresponding masses  $m_i$  ( $i = 0, 1, 2$ ). It is  
 163 important to remark that the central core  $Z_0$  and the two layers  $Z_1$  and  $Z_2$   
 164 need not to be spherical, i.e. the macroscopic model may be used to describe  
 165 not only MTS’s, but also almost any kind of pre-vascular *in vivo* solid cancers.

166 Since energy is transported to the tumor cells by the diffusing nutrients, we  
 167 assume that it is proportional to the amount of the latter. Therefore, applying  
 168 the law of energy conservation as in Ref. (Delsanto et al., 2004), we may write  
 169 the energy balance for region  $Z_2$  as,

$$170 \quad B_2 dt = N_2 \xi_2 dt + \epsilon dN_2 + \chi dN_2 \quad (4)$$

171 where

$$172 \quad \chi = \left( \frac{\kappa P M}{\zeta} \right) \quad (5)$$

173 and  $N_2$  is the total number of cancer cells in  $Z_2$  at time  $t$ ,  $P$  is the hydrostatic  
 174 pressure on the spheroid wall,  $B_2$  is the net nutrient-associated energy inflow  
 175 into  $Z_2$  during the interval  $dt$ ,  $\zeta$  is the mass density, assumed to be uniform,  
 176  $\xi_2$  is the metabolic rate for a single cancer cell, and  $\epsilon$  is the energy required  
 177 to create a new cell in a “soft” environment. If  $M$  is the mass of a single cell,  
 178  $m_2 = MN_2$ .

179 In Eq. (4) the last term on the right-hand-side is new with respect to Ref.  
180 (Delsanto et al., 2004), and represents the amount of energy required by the  
181 volumetric expansion. It includes not only the mechanical work done by the  
182 biologically growing system against its environment at pressure  $P$ , i.e. (from  
183 thermodynamics)  $PdV_2$ , which is comparatively small (and would correspond  
184 to a value of  $\kappa = 1$ ), but also the excess energy required to create new biological  
185 material in a stressed environment. Such excess energy is the result of complex  
186 biological processes and can be assumed (at least as a first approximation) to  
187 be proportional to the volume increase,  $dV_2 = MdN_2$ .

188 Two plausible and complementary assumptions can be formulated regarding  
189 the pressure dependence, as a function of the constitutive laws of the matrix  
190 and tumor materials. In a recent paper (Guiot et al., 2006b), the interface pres-  
191 sure increases due to the tumor elastic growth, until a characteristic strength  
192 of the matrix is reached, the stress released and a new annular region of matrix  
193 colonized by the tumor. In this model a perfectly plastic constitutive law for  
194 the matrix is also assumed, corresponding to a strain flow at a given value  
195  $P$ . For such a case the pressure  $P$  is expected to be constant, representing  
196 the yielding strength of the matrix material. Obviously these two assumptions  
197 represent limit conditions of a more complex reality, but the introduction of  
198  $P$  represents an important novelty with respect to previous models (for which  
199  $P = 0$ ), due to the role of mechanical stress in triggering and controlling var-  
200 ious biomechanical and biophysical processes (Chaplain , 2006) both at the  
201 single cell level (remodulation of intracellular structures by the cell deforma-  
202 tion and consequent change in gene expression and protein synthesis (Ingber  
203 et al., 1995) and at the multicellular one (change of intercellular communica-  
204 tions via release of molecules, apoptosis and cell proliferation control via the  
205 change of cell adhesion (Shraiman , 2005; Hufnagel et al., 2007; Helmlinger

206 et al., 1997)).

207 The left-hand-side of Eq. (4),  $B_2 dt$ , describes the energy necessary for the  
 208 overall thermodynamic processes occurring within the cell population occupy-  
 209 ing the region  $Z_2$ . This energy, as previously stated, results from the balance  
 210 of two different flows of nutrients molecules (the carriers of energy for every  
 211 metabolic process): the total diffusive inflow towards the spheroid, which is  
 212 proportional to a power  $p_2$  of its whole mass, according to the general law  
 213 relating the mass of a biological system and the rate of energy inflow needed  
 214 for maintenance and proliferation (West et al., 1999, 2001; Guiot et al., 2003),  
 215 and the nutrient molecules flow towards the inner region  $Z_1$ , which produces  
 216 an energy leakage rate for the  $Z_2$  population, but an energy acquisition rate  
 217 for the  $Z_1$  one proportional to the  $p_1$  power of its mass, according to the same  
 218 law. Thus,

$$219 \quad B_2 = B_{02}(m_0 + m_1 + m_2)^{p_2} - B_{01}(m_0 + m_1)^{p_1}, \quad (6)$$

220 where  $B_{01}$  and  $B_{02}$  are constants. The assumption that cellular feeding is  
 221 controlled only by diffusive processes, i.e. that the tumor is in a pre-vascular  
 222 stage, would imply that  $p_1 = p_2 = 2/3$ , because the inflow through the sur-  
 223 face is proportional to the  $2/3$  power of the volume. By contrast WBE's law  
 224 assumes that resources are transported to the cells through a fractal hierar-  
 225 chical branching network (West et al., 1999), which implies  $p = 3/4$ . In fact,  
 226 the power law dependence of  $B$  on  $m$  has been recognized for a long time  
 227 (Kleiber, 1932), but the value of the exponent and its ultimate meaning are  
 228 still sources of controversy (Dodds et al., 2001; Makarieva et al., 2003). It has  
 229 been recently pointed out that our model (and in particular a careful moni-  
 230 toring of the  $p$  exponent) may enable us to predict the progression of a tumor  
 231 (Guiot et al., 2006a; Carpinteri and Pugno, 2005; Guiot et al., 2006b).

232 On heuristically justified grounds, we can also apply the same formulation  
 233 to describe cell evolution in  $Z_0$  and  $Z_1$ , using the same approach and the same  
 234 type of rules which connect the energy rate consumed by a cell population to  
 235 its total mass through a power law. By extending the definition of  $B_{02}$  and  $\xi_2$   
 236 to the other two regions and using Eqs. 4 and 6, the subsequent equation for  
 237 the temporal evolution of the masses of each cell population is obtained:

$$238 \quad \frac{dm_i}{dt} = a_i \left( \sum_{j=0}^i m_j \right)^{p_i} - a_{i-1} \left( \sum_{j=0}^{i-1} m_j \right)^{p_{i-1}} - b_i m_i, \quad (7)$$

239 where  $m_i$  is the total mass of the  $i$ -th population, for  $i = 0, 1, 2$ , and

$$240 \quad a_i = \frac{MB_{0i}}{\epsilon + \kappa PM/\zeta}, \quad (8)$$

$$241 \quad b_i = \frac{\xi_i}{\epsilon + \kappa PM/\zeta}, \quad (9)$$

242 with  $a_{-1} = 0$ . The growth of the tumor mass in each region is proportional  
 243 to the difference between the net energy input (first term minus second term  
 244 in Eq. 7 and the amount of energy used for cell maintenance (third term).  
 245 Equations (7) to (9) define a consistent phenomenological model whose pa-  
 246 rameters may be evaluated from the results of macroscopic experiments. They  
 247 belong to a class, called U2, of a recently proposed classification scheme for  
 248 phenomenological universalities in growth problems (Castorina et al., 2006).  
 249 U2 includes, as special cases, the WBE, the logistic and all the other previ-  
 250 ously proposed growth models. The introduction of the expansion term in Eq.  
 251 (4) leads to a reduction in the size of most of the coefficients, a fact whose  
 252 consequences will be explored later. The outer shell coefficients  $a_2$  and  $b_2$  can  
 253 be obtained from experimental observations of the whole spheroid (Condat  
 254 and Menchón, 2006). As indicated in the Appendix, the coefficients  $a_0$  and  $b_0$   
 255 can be obtained from observations of the necrotic core.

256 If we assume that necrotic cells do not consume energy  $\xi_0 = 0$ . Then  $b_0 = 0$   
 257 and Eq. (7) for  $m_0$  can be straightforwardly solved, yielding,

$$258 \quad m_0(t) = [(\tilde{m})^{1-p_0} + a_0(1-p_0)(t-t_0)]^{1/(1-p_0)} \quad (10)$$

259 where  $p_0 \neq 1$  and  $\tilde{m}$  is the mass at time  $t_0$ . If we choose  $t_0$  as the time of  
 260 onset of the necrotic core,  $\tilde{m} = 0$ . At long times the necrotic mass increases  
 261 as a power law; in particular, if  $p_0 = 2/3$ ,  $m_0(t) \sim t^3$ . For  $p_0 = 1$ , there is ex-  
 262 ponential growth at all times. Since  $a_0$  is expected to decrease with increasing  
 263 pressure, the necrotic core (and the rest of the tumor) will grow more slowly  
 264 under conditions of higher pressure. A tumor steady state can be obtained  
 265 from Eqs. (7) only if  $b_0 \neq 0$ .

#### 266 4 THE BRIDGE: INTERMEDIATE MODEL

267 To formulate an auxiliary model that allows us to bridge the gap between the  
 268 mesoscopic and macroscopic descriptions, we start by rewriting the equation  
 269 describing the evolution of the number of cancer cells in the  $n^{th}$  mesoscopic  
 270 shell as a first order differential equation that explicitly exhibits the cell fluxes.  
 271 Assuming that the time step  $\tau$  is very small, we write,

$$272 \quad c_n^* - c_n \approx \tau \frac{dc_n}{dt} \quad (11)$$

273 The mesoscopic Eq.(1) then becomes

$$274 \quad \frac{dc_n}{dt} = \beta_n c_n + \Phi_{n-1} - \Psi_{n-1} + \Psi_n - \Phi_n, \quad (12)$$

275 where  $\Phi_n$  and  $\Psi_n$  stand for the outward and inward cell flows, respectively

$$\Phi_n = (n+1)^{2/3} r_0^2 \mu_n^+ c_n, \quad (13)$$

$$\Psi_n = (n+1)^{2/3} r_0^2 \mu_{n+1}^- c_{n+1}, \quad (14)$$

276 where  $\beta_n = \rho_n - \delta_n$  is the difference between the reproduction and death  
 277 rates, except in  $Z_0$  where  $\beta_n = -\lambda_n$ .

278 Next we regroup the shells with  $n \leq n_0$ ,  $n_0 < n \leq n_1$  and  $n_1 < n \leq n_2 = N$   
 279 in the three regions,  $Z_0$ ,  $Z_1$  and  $Z_2$ , respectively. Although the equation de-  
 280 scribing the nutrient evolution in the mesoscopic model (Eq. 3) is not explic-  
 281 itly considered, the role of the nutrient distribution is clear: since the nutrient  
 282 comes from outside and is progressively consumed (or stored for later con-  
 283 sumption) by the viable cells inside, the above stratification is a reasonable  
 284 approximation (Mueller-Klieser, 2000). Of course, due to the randomness in-  
 285 herent to the involved processes, we would expect a smoother distribution in  
 286 the experimental data.

287 In order to set the model in a form adequate for the comparison, we proceed  
 288 as follows:

289 1. At each discretization step we will conceptually separate the description  
 290 of growth into two stages. In the first stage cells multiply, migrate and die, but  
 291 the volumes of the various zones are kept constant. In the second stage, the  
 292 zone radii are allowed to vary in order to restore cell concentration uniformity.  
 293 Therefore the rescaled zone volumes “recapture” the cells that left each zone  
 294 during the first step; this corresponds to a loss of mass  $-dm_i$  for the zone  $Z_i$ .

295 2. Since we are solely interested in the number of cells inside each region,  
 296 we can sum over the contributions of all its shells. Internal migrations in each  
 297 region do not affect the number of cells therein and are therefore irrelevant.  
 298 The only migration terms that matter are those across the region boundaries,  
 299 that is to the shells  $n = n_0$ ,  $n_1$  and  $n_2 = N$ .

300 3. By definition, all cells are included in the MTS; thus, no cells can enter  
 301 from the outside:  $\Psi_{n_2} = 0$ . We will disregard the centripetal migrations  $\Psi_{n_0}$   
 302 and  $\Psi_{n_1}$  since they would amount to including active cells in  $Z_1$  or quiescent

ones in  $Z_0$  (which is forbidden by our definition of the regions). Operationally,  
 this implies setting the transport coefficients  $\mu_{n_i}^- = 0$  at the region edges.  
 Alternatively, we may redefine  $\bar{\Phi}_n$  as the net balance  $\Phi_n - \Psi_n$ .

4. As a coarse grain approximation, the rates  $\delta_n$ ,  $\rho_n$  and  $\lambda_n$  may be rea-  
 sonably equated in each region to their asymptotic values or to 0 as a conse-  
 quence of the sigmoidal functions implementing their dependence from nutri-  
 ent concentrations. This corresponds to selecting very steep sigmoidal func-  
 tions (Griffa et al., 2004). It follows that  $\delta_n = \rho_n = 0$  in the first (necrotic)  
 region, since dead cells cannot die or reproduce; we also fix  $\lambda_n = \lambda$  in the  
 same region. In  $Z_1$  we set  $\delta_n = \delta$  and  $\rho_n = 0$ , while in  $Z_2$  we write  $\delta_n = 0$  and  
 $\rho_n = \rho$ , with both  $\rho$  and  $\delta$  being the asymptotic values of the corresponding  
 variables.

With the above assumptions, we can use the set of Eqs. (12) to obtain  
 equations for the total numbers of cells  $\bar{c}_i = \sum c_j$  in their respective regions  
 $Z_i$  ( $i = 0, 1, 2$ ). Summing Eqs. (12) over  $n$  for all the shells included in each of  
 the three regions  $Z_i$ , we obtain

$$\frac{d\bar{c}_2}{dt} = \rho\bar{c}_2 + \bar{\Phi}_{n_1} - \bar{\Phi}_{n_2}, \quad (15)$$

$$\frac{d\bar{c}_1}{dt} = -\delta\bar{c}_1 + \bar{\Phi}_{n_0} - \bar{\Phi}_{n_1}, \quad (16)$$

$$\frac{d\bar{c}_0}{dt} = -\bar{\Phi}_{n_0} - \lambda\bar{c}_0, \quad (17)$$

The outward cell flux from the outermost shell of each region  $Z_i$  ( $i = 0, 1, 2$ )  
 across the surface separating it from the next region (the matrix in the case  
 $i = 2$ ) can be renamed as  $\bar{\Phi}_i$ :  $\bar{\Phi}_0 = \bar{\Phi}_{n_0}$ ,  $\bar{\Phi}_1 = \bar{\Phi}_{n_1}$  and  $\bar{\Phi}_2 = \bar{\Phi}_{n_2}$ , where  $n_2 = N$ .

In Eq. (16)  $\delta\bar{c}_1$  is the total dying cell rate. Since cells in the necrotic core  
 may only be reabsorbed, the only contributions to cell variation in  $Z_0$  are  
 given by the flux  $-\bar{\Phi}_0$  and the absorption  $-\lambda\bar{c}_0$ .

328 Next we evaluate the fluxes  $\bar{\Phi}_i$ . The factor  $r_0^2(n+1)^{2/3}$  in Eqs. (13) and (14),  
 329 for  $n = n_i$  ( $i = 0, 1, 2$ ), corresponds to the square of the external radius,  $R_i^2$ , of  
 330 the corresponding zone,  $Z_i$ . Because migrations to other regions start only from  
 331 the outermost shell in each region, the fluxes will be proportional to  $\eta\mu_i$  ( $i =$   
 332  $0, 1, 2$ ), where  $\mu_i \equiv \mu_{n_i}^+$  is the local mobility and  $\eta = c_{n_i}$  is the mean number  
 333 of cells in the  $n_i$ -th isovolumetric shell. We keep  $\eta$  approximately constant  
 334 because of the migration mechanism based on the mechanical stress-driven  
 335 mass transport. In fact the outer shell of each zone is subject to an outwards  
 336 chemotaxis-based cell migration due to the gradient in the concentration of  
 337 nutrients (Dorie et al., 1982, 1986; McElwain and Pettet, 1993) (which tends  
 338 to increase local cell density), but also to the mechanical opposition of the  
 339 external cells (or the extracellular matrix in the case of the proliferant rim  $Z_2$ ).  
 340 The intermediate increase of cell density is then compensated by the stress-  
 341 driven migration (invasion in the case of the proliferative rim), in order not to  
 342 increase the cell density above its maximum allowed value (Deisboeck et al.,  
 343 2005). The constant cell density assumption in the formulation of the IM is  
 344 in agreement with many experimental observations ( (Freyer and Sutherland,  
 345 1986b, 1985, 1980)), although other recent investigations (Nirmala et al., 2001)  
 346 show that it may slightly vary in time and space due to the local heterogeneities  
 347 at smaller scales within the MTS. The fluxes can be written as,

$$348 \quad \bar{\Phi}_i = \mu_i c_{n_i} R_i^2 = \mu_i \eta \left( \frac{3}{4\pi\zeta} \sum_{j=0}^i m_j \right)^{2/3}. \quad (18)$$

349 Next, we correlate Eqs. (7) for the mass variations with Eqs.(15-17) for the  
 350 variations in cell numbers. Using the two-stages model at each discretization  
 351 step, as discussed before, from  $m_i = M\bar{c}_i$ , it follows

$$352 \quad \frac{d\bar{c}_i}{dt} = -\frac{1}{M} \frac{dm_i}{dt} \quad (19)$$

353 Now we can combine Eqs. (15) to (19) to write the equations for the mass  
354 variations in each of the three zones:

$$\frac{dm_2}{dt} = -\rho m_2 - \sigma \mu_1 (m_0 + m_1)^{2/3} + \sigma \mu_2 (m_0 + m_1 + m_2)^{2/3}, \quad (20)$$

$$\frac{dm_1}{dt} = -\delta m_1 - \sigma \mu_0 m_0^{2/3} + \sigma \mu_1 (m_0 + m_1)^{2/3}, \quad (21)$$

355 and

$$\frac{dm_0}{dt} = -\lambda m_0 + \sigma \mu_0 m_0^{2/3}, \quad (22)$$

357 where

$$\sigma = M\eta \left( \frac{4\pi}{3} \zeta \right)^{-2/3}. \quad (23)$$

359 By comparing Eqs. (7) with Eqs. (20)-(22), we find that both models coin-  
360 cide if the following parameter identification is performed:

$$a_0 = \sigma \mu_0, \quad a_1 = \sigma \mu_1, \quad a_2 = \sigma \mu_2, \quad (24)$$

$$b_0 = -\lambda, \quad b_1 = -\delta, \quad b_2 = \rho \quad (25)$$

361 and

$$p_0 = p_1 = p_2 = 2/3 \quad (26)$$

363 We have thus related the parameters corresponding to the mesoscopic and  
364 macroscopic formulations. That  $p_i = 2/3$  was to be expected by the con-  
365 struction of the mesoscopic model, but the other relations provide us with  
366 information about the dependence of the mesoscopic parameters on pressure.  
367 For instance, the interzone migration fluxes must decrease with increasing  
368 pressure,

$$\mu_i = \frac{MB_{0i}}{\sigma \left( \epsilon + \frac{\kappa PM}{\zeta} \right)}. \quad (27)$$

370 This is reasonable, because migration is hindered by the increased cell con-  
 371 centration. The reproduction rate is decreased by the same factor:

$$372 \quad \rho = \frac{\xi_2}{\epsilon + \frac{\kappa PM}{\zeta}}, \quad (28)$$

373 which is also consistent with predictions put forward on the basis of exper-  
 374 imental data (Helmlinger et al., 1997). Since it is not a priori clear what the  
 375 dependence of  $b_0$  and  $b_1$  on  $P$  should be, we cannot draw general conclusions  
 376 on the mesoscopic coefficients  $\lambda$  and  $\delta$ . However, if we assume that the depen-  
 377 dence of  $b_1$  on  $P$  is the same as that of  $b_2$ , then we can conclude that the death  
 378 rate is decreased by increasing pressure, a somewhat surprising result, which  
 379 however, agrees with the results of Helmlinger and co-workers, who observed  
 380 that solid mechanical stress decreases the apoptotic rate (Helmlinger et al.,  
 381 1997). This decrease in the apoptotic rate is likely to be due to increased  
 382 packing and concomitantly enhanced cell-cell interactions, which trigger the  
 383 suppression of apoptotic cell death. Moreover,  $\delta > 0$  implies  $b_1 < 0$ , that is,  
 384 the proliferating - to - quiescent bulk transformation is faster than the quies-  
 385 cent - to - dead bulk transformation. Similarly,  $\lambda > 0$  implies that the bulk  
 386 dying rate must be larger than the reabsorption rate.

## 387 5 CONCLUSIONS

388 Through the introduction of an intermediate model, we have proved the  
 389 consistency of two very different models for heterogeneous MTS growth: a  
 390 macroscopic model, based on the ontogenetic growth model of West, Brown  
 391 and Enquist, and a mesoscopic one, based on the coarse-graining of the cell  
 392 system. Besides its intrinsic importance as a bridging tool, this unification  
 393 helps us to establish a correspondence between hard-to-measure microscopic

394 parameters and their more accessible macroscopic counterparts (see e.g. Fig.  
395 3).

396 The correspondence between the two models is remarkable, since they stem  
397 from completely different approaches, as stated in the Introduction. It is im-  
398 portant to note that:

399 1. The IM model in its present form is not self-standing, i.e. it cannot by  
400 itself be used for actual simulations, since it implicitly depends on the evolving  
401 nutrient distribution (provided by the Eq. (3) in the mesoscopic model).

402 2. The consumption rate of nutrients due to the metabolism, which is ex-  
403 plicit in the mesoscopic model is only implicit in the IM, via the “ignored”  
404 Eq. 3. Thus the metabolism parameters  $b_i$  correspond to the “cell activity”  
405 parameters in  $\beta_i$  in the IM.

406 3. According to Eqs. (20) to (22), the parameters  $p_i$  are all equal to  $2/3$ ,  
407 which indicates that feeding must be diffusion-controlled to ensure consistency  
408 between the models. However, the values of the parameters  $p_i$  depend on the  
409 nature of nutrient transport. For instance, MTS internal vascularization is  
410 likely to change their values.

411 The present treatment lends itself to suggest, through simulations and math-  
412 ematical analysis, the relevance of the effects of different tumor microenviron-  
413 nments, some of which are easier to study *in vitro* or by implanting MTS in  
414 model laboratory animals (Oudar, 2000). For example, we could extend it to  
415 the case of underfeeding (Delsanto et al., 2004; Griffa and Scalerandi, 2005)  
416 and to the development of angiogenesis. In the latter case, it would be useful  
417 to find a connection between the various extant mesoscopic model (Dodds  
418 et al., 2001; Byrne and Chaplain, 1995; Byrne et al., 2006), and the simple  
419 predictions about the dependence of the growth rate on the instantaneous  
420 mass furnished by the macroscopic approach (Menchón and Condat, 2007).

421 One could also explicitly consider the presence of growth inhibitors or consider  
422 the role of the necrotic mass in regulating the number of viable quiescent cells  
423 at the interface between the  $Z_0$  and  $Z_1$  regions. It is well known that necrotic  
424 death is closely related to the release of cytotoxic intra-cellular substances in  
425 the extra-cellular microenvironment (Greenspan, 1974; Freyer, 1988; Groebe  
426 and Mueller-Klieser, 1996). This process deserves to be considered with care.  
427 To conclude, we have used the simplest possible form for the dependence of  
428 the extra term in the WBE equation on the pressure. Our results could be  
429 easily generalized to more complicated cases by replacing  $\kappa P$  in Eq. (4) with  
430 a suitable positive, monotonically increasing function  $F(P)$ . This would not  
431 introduce any qualitative changes in the results obtained here. Finally, we  
432 must remark that in our model the growth process is controlled by nutrient  
433 consumption and the possible influence of growth promoters/inhibitors is ne-  
434 glected. We also have neglected part of the cell-cell interactions and cell-cycle  
435 details (Jiang et al., 2005).

### 436 **Acknowledgements**

437 This work was supported in part by CONICET (Argentina), through PIP  
438 6311/05, by SECyT-UNC (Argentina). One of us (PPD) wishes to thank Prof.  
439 C. Guiot for useful discussions. P.P. Delsanto, M. Griffa and A. Gliozzi would  
440 like to acknowledge the support received within the stimulating framework of  
441 the NIH-NCI Integrative Cancer Biology Program CViT Project and by the  
442 collaboration with the Bioinformatics and High Performance Computing Lab  
443 of the Bioindustry Park of Canavese (Colleretto Giacosa, Torino, Italy).

444 **FIGURE CAPTIONS**

445 **Fig.1:** Schematic representation of the basic cellular processes in the n-th  
 446 MTS shell as a function of the number of available nutrient units  $\nu_n$ . The three  
 447 lines below the  $\nu_n$  axis imply that cellular death occurs only for  $\nu_n < Q_D$ ,  
 448 migration for  $\nu_n < Q_M$  and cell reproduction for  $\nu_n > Q_R$ , respectively.  
 449 Correspondingly, the three parameters  $\delta_n$ ,  $\mu_n$  and  $\rho_n$  are different from zero  
 450 (and equal to  $\delta, \mu$  and  $\rho$ ) only for  $\nu_n < Q_M$ ,  $\nu_n < Q_M$  and  $\nu_n > Q_R$ ,  
 451 respectively.

452 **Fig. 2:** The three stages of development of a MTS, as obtained from a  
 453 mesoscopic simulation at three successive times. In the first stage all cells are  
 454 proliferating. In the second one a region of quiescent cells emerges and soon  
 455 occupies most of the interior. In the third one a necrotic core develops, which,  
 456 however, includes some viable cells in the process of dying (especially at its  
 457 rim). The mesoscopic parameters for the simulations are  $\mu = 0.003$ ,  $\rho = 0.025$ ,  
 458  $\delta = 0.01$ ,  $\sigma = 1.7$  in the nonzero zone defined in Fig.1.

459 **Fig. 3:** Comparison between the results of a macroscopic (dashed line) and a  
 460 mesoscopic (full dots) simulation with the experimental data (empty squares,  
 461 ref. (Freyer and Sutherland, 1986a)) referring to a MTS made of EMT6/Ro  
 462 mouse mammary carcinoma cells grown in a culture medium. The parameters  
 463 for the macroscopic simulations are:  $a_1 = 0.15$ ,  $a_2 = 0.48$ ,  $a_3 = 0.59$ ,  $b_0 =$   
 464  $-0.012$ ,  $b_1 = 0.0016$ ,  $b_2 = 0.037$ ; the mesoscopic parameters are the same as  
 465 in Fig.2.

466 **References**

- 467 J.A. Adam and N. Bellomo, editors, *A Survey of Models for Tumor-Immune*  
468 *System Dynamics*, Birkhauser, (1996).
- 469 T. Alarcón, H.M. Byrne, P.K. Maini, A multiple scale model for tumor growth,  
470 *SIAM Multiscale Model. Simul.*, **3**, 440, (2005).
- 471 H.M. Byrne, M.A.J. Chaplain, Mathematical models for tumour angiogenesis:  
472 numerical simulations and nonlinear wave solutions, *Bull. Math. Biol.*, **57**,  
473 461, (1995).
- 474 H.M. Byrne, T. Alarcon, M.R. Owen, S.D. Webb, P.K. Maini, Modelling as-  
475 pects of cancer dynamics: a review, *Phil. Trans. Roy. Soc. A*, **364**, 1563,  
476 (2006).
- 477 A. Carpinteri and N. Pugno, Are the scaling laws on strength of solids related  
478 to mechanics or to geometry?, *Nature mat.*, **4**, 421, (2005).
- 479 P. Castorina, P.P. Delsanto, and C. Guiot, Classification scheme for phe-  
480 nomenological universalities in growth problems in physics and other sci-  
481 ences, *Phys. Rev. Lett.*, **96**, 188701, (2006).
- 482 M.A.J. Chaplain, L. Graziano and L. Preziosi, Mathematical modelling of  
483 the loss of tissue compression responsiveness and its role in solid tumour  
484 development, *Math. Med. Biol.*, **23**, 197-229, (2006).
- 485 W.Y. Chen, P.R. Annamreddy, and L.T. Fan, Modeling growth of heteroge-  
486 neous tumor, *J. Theor. Biol.*, **221**, 205, (2003).
- 487 R. Chignola, A. Schenetti, E. Chiesa, R. Foroni, S. Sartoris, A. Brendolan,  
488 G. Tridente, G. Andrighetto, and L. Liberati, Forecasting the growth of  
489 multicell tumour spheroids: implication for the dynamic growth of solid  
490 tumours, *Cell Prolif.*, **33**, 219, (2000).
- 491 C.A. Condat and S.A. Menchón, Ontogenetic growth of multicellular tumor

- 492 spheroids, *Physica A*, **371**, 76, (2006).
- 493 V. Cristini, H.B. Frieboes, R. Gatenby, S. Caserta, M. Ferrari, J. Sinek, Mor-  
494 phological instability and cancer invasion, *Clin. Cancer Res.*, **11**, 6772,  
495 (2005).
- 496 T.S. Deisboeck, Y. Mansury, C. Guiot, P.G. Degiorgis, and P.P. Delsanto, In-  
497 sights from a novel tumor model: Indications for a quantitative link between  
498 tumor growth and invasion, *Med. Hypotheses*, **65**, 785, (2005).
- 499 P.P. Delsanto, R. Mignogna, M. Scalerandi, R. Schechter, in *New Perspectives*  
500 *on Problems in Classical and Quantum Physics*, edited by P. P. Delsanto  
501 and A. W. Saenz (Gordon & Breach, New Delhi, 1998), Vol. 2, pp. 5174.
- 502 P.P. Delsanto, C. Guiot, P.G. Degiorgis, C.A. Condat, Y. Mansury, and  
503 T. Deisboeck, Growth model for multicellular tumor spheroids, *Appl. Phys.*  
504 *Lett.*, **85**, 4225, (2004).
- 505 P.P. Delsanto, M. Griffa, C.A. Condat, S. Delsanto, and L. Morra, Bridging the  
506 gap between mesoscopic and macroscopic models: the case of multicellular  
507 tumor spheroids, *Phys. Rev. Lett.*, **94**, 148105, (2005a).
- 508 P.P. Delsanto, L. Morra, S. Delsanto, M. Griffa, and C. Guiot, Towards a  
509 Model of Local and Collective Mechanisms in Multicellular Tumor Spheroids  
510 Growth, *Physica Scripta*, **T118**, 157, (2005b).
- 511 M. Dembo and Y.L. Wang, Stresses at the cell-to-substrate interface during  
512 locomotion of fibroblasts, *Biophys. J.*, **76**, 2307, (1999).
- 513 S. Dodds, D.H. Rothman, and J.S. Weitz, Re-examination of the 3/4-law of  
514 metabolism, *J. Theor. Biol.*, **209**, 9, (2001).
- 515 M.J. Dorie, R.F. Kallman, D.F. Rapacchietta, D. Van Antwerp, Y. Rong  
516 Huang, Migration and internalization of cells and polystyrene microspheres  
517 in tumour cell spheroids, *Exp. Cell Res.*, **141**, 201, (1982).
- 518 M.J. Dorie, R.F. Kallman, M.A. Coyne, Effect of cytochalasin B, nocodazole

- 519 and irradiation on migration and internalization of cells and microspheres  
520 in tumor cell spheroids, *Exp. Cell Res.*, **166**, 370, (1986).
- 521 S. C. Ferreira, M.L. Martins, and M.J. Vilela, Reaction-diffusion model for  
522 the growth of avascular tumor, *Phys. Rev. E*, **65**, 021907, (2002).
- 523 J.P. Freyer, Role of necrosis in regulating the growth saturation of multicellular  
524 spheroids, *Cancer Res.*, **48**, 2432, (1988).
- 525 J.P.Freyer and R.M. Sutherland, Selective dissociation and characterization of  
526 cells from different regions of multicell tumor spheroids, *Cancer Res.*, **40**,  
527 3956, (1980).
- 528 J.P.Freyer and R.M. Sutherland, A reduction in the in situ rates of oxygen  
529 and glucose consumption of cells in EMT6/Ro spheroids during growth, *J.*  
530 *Cell Phys.*, **124**, 516, (1985).
- 531 J.P.Freyer and R.M. Sutherland, Regulation of growth saturation and devel-  
532 opment of necrosis in EMT6/Ro multicellular spheroids by the glucose and  
533 oxygen supply, *Cancer Res.*, **46**, 3504, (1986a).
- 534 J.P.Freyer and R.M. Sutherland, Proliferative and clonogenic heterogeneity  
535 of cells from EMT6/Ro multicellular spheroids induced by the glucose and  
536 oxygen supply, *Cancer Res.*, **46**, 3513, (1986b).
- 537 H.B. Frieboes, X. Zheng, Ch.-H. Sun, B. Tromberg, R. Gatenby, V. Cristini,  
538 An integrated computational/experimental model of tumor invasion, *Can-*  
539 *cer Res.*, **66**, 1597, (2006).
- 540 V.D. Gordon, M.T. Valentine, M.L. Gardel, D. Andor, S. Dennison, A.A.  
541 Bogdanov, D.A. Weitz, T.S. Deisboeck, Measuring the mechanical stress  
542 induced by an expanding multicellular tumor system: a case study, *Exp.*  
543 *Cell Res.*, **289**, 58, (2003).
- 544 H.P. Greenspan. On the self-inhibited growth of cell cultures. *Growth*, **38**, 81,

- 545 (1974).
- 546 M. Griffa and M. Scalerandi, Physical modeling and simulations of tumor  
547 growth and angiogenesis: predictions and new hypotheses, *Physica Scripta*,  
548 **T118**, 183, (2005).
- 549 M. Griffa, S. Delsanto, L. Morra, and P.P. Delsanto, Mesoscopic Modeling  
550 of Multicellular Tumor Spheroids: Validation through a Quantitative Com-  
551 parison with Experimental Data, *WSEAS Transactions on Biology and*  
552 *Biomedicines*, **1**, 249, (2004).
- 553 K. Groebe and W. Mueller-Klieser, On the relation between size of necrosis  
554 and diameter of tumor spheroids, *Int. J. Rad. Oncol. Biol. Phys.*, **34**, 395,  
555 (1996).
- 556 C. Guiot, P.G. Degiorgis, P.P. Delsanto, P. Gabriele, and T.S. Deisboeck, Does  
557 Tumor Growth Follow a Universal Law?, *J. Theor. Biol.*, **225**, 147, (2003).
- 558 C. Guiot, P.P. Delsanto, A. Carpinteri, N. Pugno, Y. Mansury, and T.S. Deis-  
559 boeck, The dynamic evolution of the power exponent in a universal growth  
560 model of tumors, *J. Theor. Biol.*, **240**, 459, (2006a).
- 561 C. Guiot, N. Pugno, and P.P. Delsanto, An elastomechanical model for tumor  
562 invasion, *Applied Physics Letters*, **89**, 1, (2006b).
- 563 G. Hamilton, Multicellular spheroids as an *in vitro* tumor model, *Cancer Lett.*,  
564 **131**, 29, (1998).
- 565 G. Helmlinger, P.A. Netti, H.C. Lichtenbed, R.J. Melder, and R.K. Jain, Solid  
566 stress inhibits the growth of multicellular tumor spheroids, *Nature Biotech.*,  
567 **15**, 778, (1997).
- 568 L. Hufnagel, A.A. Teleman, H. Rouault, S.M. Cohen, B.I. Shraiman, On the  
569 mechanism of wing size determination in fly development, *Proc. Natl. Acad.*  
570 *Sci. USA*, **104**, 3835, (2007).
- 571 D.E. Ingber, D. Prusty, Z. Sun, H. Betensky, N. Wang, Cell shape, cytoskeletal

- 572 mechanics, and cell cycle control in angiogenesis, *J. Biomech.*, **28**, 1471,  
573 (1995).
- 574 J.M. Kelm, N.E. Timmins, C.J. Brown, M. Fussenegger, and L.K. Nielsen,  
575 Method for generation of homogeneous multicellular tumor spheroids appli-  
576 cable to a wide variety of cell types, *Biotech. And Bioeng.*, **83**, 173, (2003).
- 577 M. Kleiber, Body size and metabolism, *Hilgardia*, **6**, 315, (1932).
- 578 Y. Jiang, J. Pjevisac,-Grbovic, Ch. Cantrell, J.P. Freyer, A Multiscale model  
579 for avascular tumor growth, *Biophys. J.*, **89**, 3884, (2005).
- 580 A.M. Makarieva, V.G. Gorshkov, and B.-L. Li, A note on metabolic rate de-  
581 pendence on body size in plants and animals, *J. Theor. Biol.*, **221**, 301,  
582 (2003).
- 583 M. Marusic, Z. Bajzer, S. Vuc-Pavlovic, and J.P. Freyer, Tumor growth *in vivo*  
584 and as multicellular spheroids compared by mathematical models, *Bull.*  
585 *Math. Biol.*, **56**, 617, (1994).
- 586 D.L.S. McElwain, G.J. Pettet, Cell migration in multicell Spheroids: swim-  
587 ming. against the tide, *Bull. Math. Biol.*, **55 (3)**, 655, (1993).
- 588 S.A. Menchón and C.A. Condat, Macroscopic Dynamics of Cancer Growth,  
589 *Eur. Phys. J. Special Topics*, **143**, 89-94, (2007).
- 590 W. Mueller-Klieser, Tumor biology and experimental therapeutics, *Crit. Rev.*  
591 *In Oncol/Hematol.*, **36**, 123, (2000).
- 592 J.D.Murray, *Mathematical Biology*, volume I Springer, 3rd edition, (2004).
- 593 C. Nirmala, J. S. Rao, A. C. Ruifrok, L. A. Langfors, and M. Obeyesekere,  
594 Growth characteristics of glioblastoma spheroids, *Int. J. Oncology*, **19**, 1109,  
595 (2001).
- 596 O. Oudar, Spheroids: relation between tumour and endothelial cells, *Crit.*  
597 *Rev. Onc./Hemat.*, **36**, 99, (2000).
- 598 A.S. Perelson and G. Weisbuch, Immunology for physicists, *Rev. Mod. Phys.*,

- 599 **69**, 1219, (1997).
- 600 L. Preziosi, editor. *Cancer Modelling and Simulation*. Chapman and  
601 Hall/CRC, (2003).
- 602 B. Capogrosso Sansone, P.P. Delsanto, M. Magnano, and M. Scalerandi, Ef-  
603 fects of anatomical constraints on tumor growth, *Phys. Rev. E*, **64**, 021903,  
604 (2001a).
- 605 M. Scalerandi, B. Capogrosso Sansone and C.A. Condat, Diffusion with evol-  
606 ving sources and competing sinks: Development of angiogenesis, *Phys. Rev.*  
607 *E*, **65**, 011902, (2001b).
- 608 M. Scalerandi and B. Capogrosso Sansone, Inhibition of vascularization in  
609 tumor growth, *Phys. Rev. Lett.*, **89**, 218101, (2002).
- 610 M. Scalerandi, A. Romano, G.P. Pescarmona, P.P. Delsanto, and C.A. Condat,  
611 Nutrient competition as a determinant for cancer growth, *Phys. Rev. E*, **59**,  
612 2206, (1999).
- 613 M. Scalerandi, B. Capogrosso Sansone, C. Benati, and C. A. Condat, Com-  
614 petition effects in the dynamics of tumor cords, *Phys. Rev. E*, **65**, 051918,  
615 (2002).
- 616 B.I. Shraiman, Mechanical feedback as a possible regulator of tissue growth,  
617 *Proc. Natl. Acad. Sci. USA*, **102**, 3318, (2005).
- 618 K.E. Thomson and H.M. Byrne, Modelling the internalization of labelled cells  
619 in tumour spheroids, *Bull. Math. Biol.*, **61**, 601, (1999).
- 620 R.B. Vernon, J.C. Angello, M.L. Iruela-Arispe, T.F. Lane, and E.H. Sage, Re-  
621 organization of basement membrane matrices by cellular traction promotes  
622 the formation of cellular networks *in vitro*, *Lab. Invest.*, **66**, 536, (1992).
- 623 G.B. West, J.H. Brown, and B.J. Enquist, The fourth dimension of life: Fractal  
624 geometry and allometric scaling of organisms, *Science*, **284**, 1677, (1999).
- 625 G.B. West, J.H. Brown, and B.J. Enquist, A general model for otogenetic

626 growth, *Nature*, **413**, 628, (2001).

Accepted manuscript

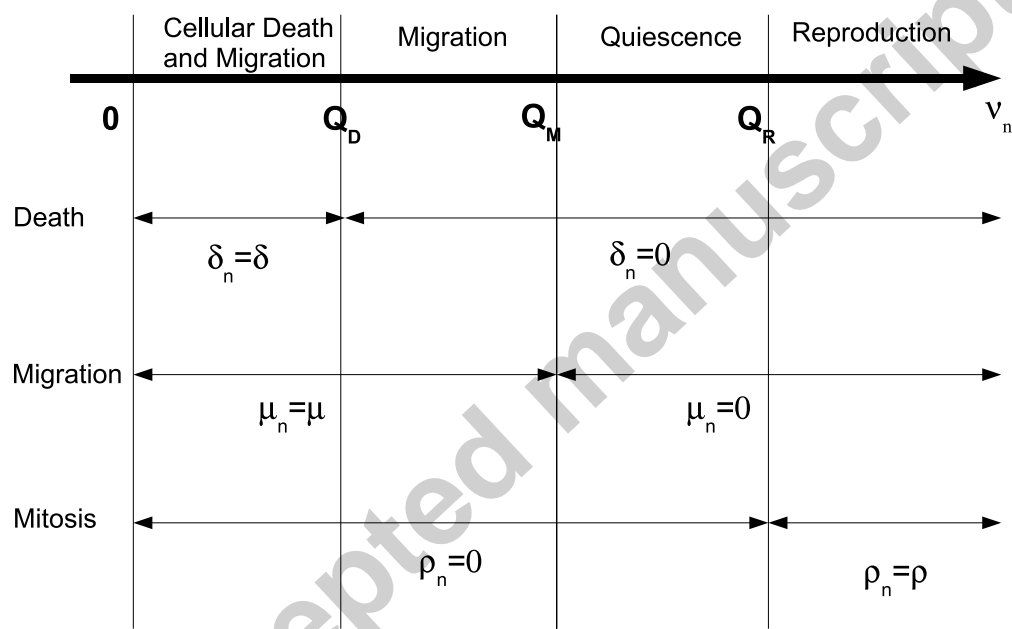


Fig. 1.

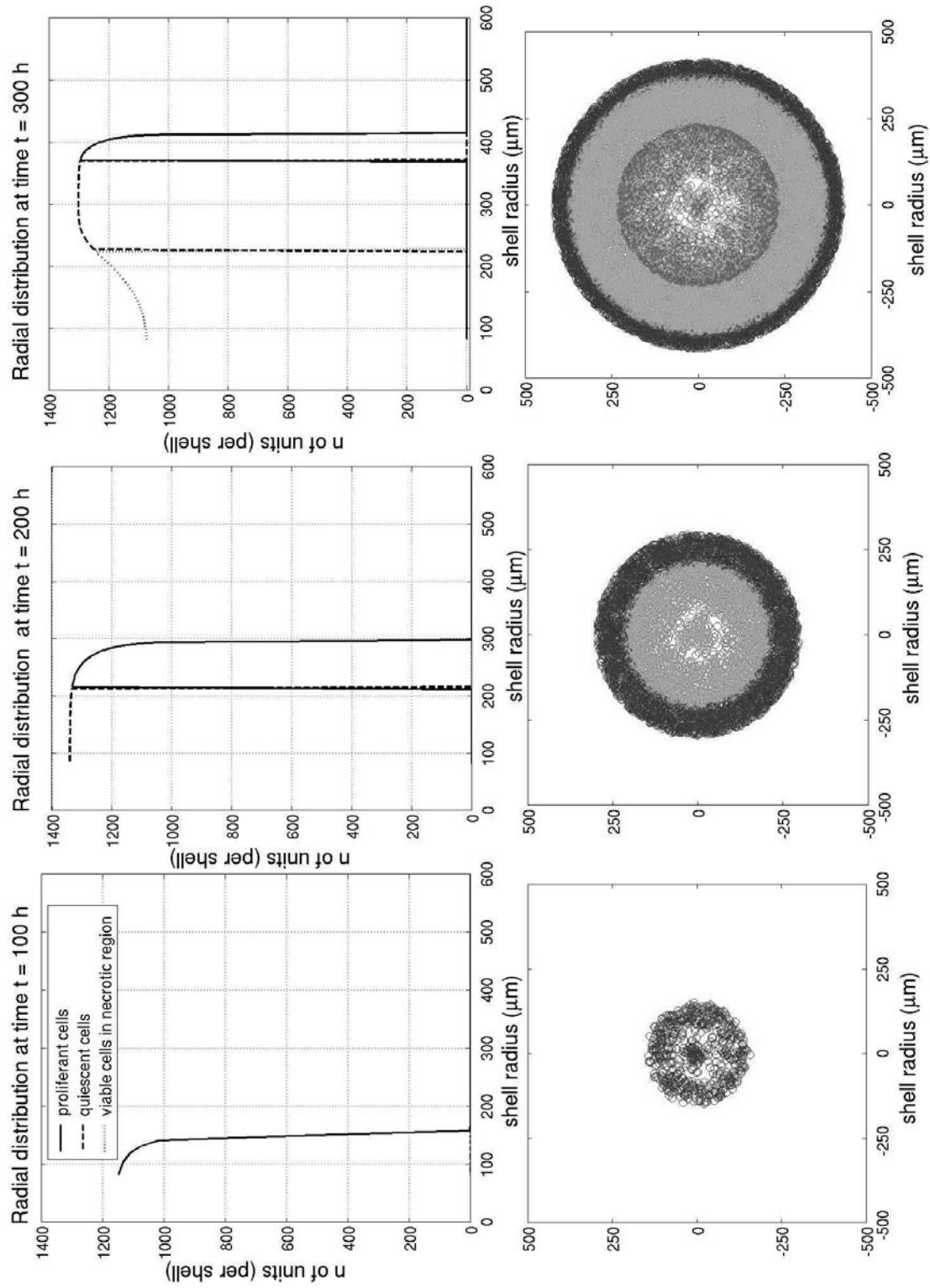


Fig. 2.

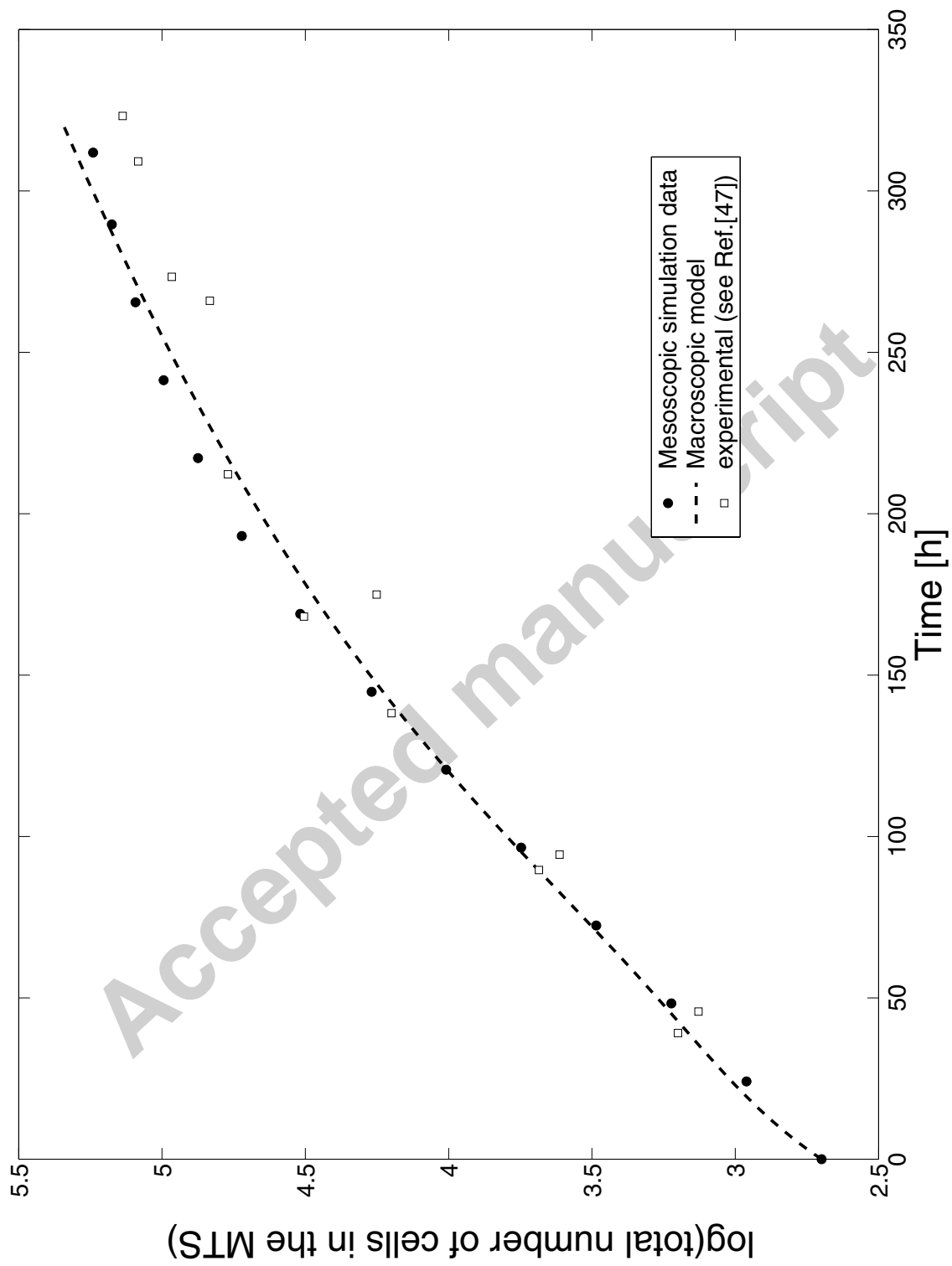


Fig. 3.